V, Nb, and Ta Complexes with Benzene in Solid Argon: An Infrared Spectroscopic and Density Functional Study

Jonathan T. Lyon and Lester Andrews*

Chemistry Department, University of Virginia, P.O. Box 400319, Charlottesville, Virginia 22904-4319

Received: September 3, 2004; In Final Form: October 29, 2004

Vanadium, niobium, and tantalum metal atoms, produced by laser ablation, are reacted with benzene vapor diluted in argon and codeposited onto a 7 K CsI window. The resulting reaction products are trapped, and the $M(C_6H_6)$ and $M(C_6H_6)_2$ complexes are identified by benzene isotopic substitution (C_6H_6, $^{13}C_6H_6$, C_6D_6). Density functional theory (DFT) frequency calculations are used to support molecular complex assignments. On the basis of the computed energies and a comparison of calculated and observed vibrational isotopic shifts, the ground electronic states and geometries are predicted. The bonding and electronic interactions in these molecules are discussed on the basis of the observed aromatic C−C breathing modes activated in the complexes.

Introduction

Since the discovery of the sandwich $V(C_6H_6)_2$ compound in 1957,[1,2] a wide variety of approaches have been used to characterize this complex. Theoretical calculations have been performed,[3−15] and a multitude of spectroscopic methods including IR,[7,16] Raman,[17] optical,[8] NMR,[18] mass and photoionization spectroscopy,[2,19−22] electron spin resonance,[8,23,24] electronic absorption,[25] electron−nuclear double resonance (ENDOR),[23,26] and photoelectron spectroscopy[24] have been used to characterize this molecule. However, less is known about the reactive $V(C_6H_6)$ complex. Theoretical methods have attempted to characterize this complex;[10,15,16,27−32] however, there is disagreement about its properties. Spin multiplicities of two,[15,16,27−29] four,[32] and six[10,31] have all been reported for the ground electronic state. With the exception of one study,[15] these calculations have all been performed with the assumption that the benzene ring does not deform and the complex has a C_{6v} symmetry. Limited work on the $V(C_6H_6)$ complex has involved an argon matrix.[16,27,29] Even less is known about the heavier niobium and tantalum−benzene complexes. The few experimental and theoretical results on these heavier metal atom−benzene complexes have focused on the sandwich bisbenzene molecules.[9,24,33]

Matrix isolation experiments have proven to be suitable for studying reactions between benzene and various molecules,[34−36] alkali metals,[37,38] halogens,[39] and transition metals.[7,16,27,29,33,40−46] IR spectroscopy was used to study the benzene molecule isolated in solid argon and krypton,[47] and the photochemistry of benzene was later studied in solid argon.[48] The IR spectrum of dibenzenechromium isolated in an argon matrix has been investigated.[41] Iron, cobalt, and nickel have been reacted with benzene in both benzene[42] and argon matrices.[43] Iron was reacted with benzene again in solid argon, and the $Fe_2(C_6H_6)$ complex was shown to be one of the products.[44] The $Nb(C_6H_6)_2$ molecule has been previously studied in an argon matrix.[33] The IR spectra of $Ti(C_6H_6)_2$ have been observed in solid argon.[45,46] A series of papers reported the vanadium and benzene reaction products in an argon matrix primarily through electron paramagnetic resonance (EPR) spectroscopy and Xα-molecular orbital (MO) theoretical calculations.[8,16,27−29,40] More recently, a partial IR spectrum of the $V(C_6H_6)_2$ compound was reported in an argon matrix.[7] However, very few of these papers have studied isotopic effects, and none of them have reported carbon-13 isotopic data.

In this paper, we present IR spectra of the reaction products of laser-ablated V, Nb, and Ta metal atoms with benzene in an argon matrix, showing that the primary products are the $M(C_6H_6)$ and sandwich $M(C_6H_6)_2$ species. We then compare our theoretical results with literature values for the $V(C_6H_6)_2$ complex, showing that our DFT calculations are able to accurately predict geometries and vibrational frequencies. Using the calculated energies and isotopic vibrational frequencies, we make comments on the possible ground electronic states of the products. This is the first report on benzene complexes to include carbon-13 isotopic substitution and a definitive assignment of the ring breathing modes.

Experimental and Computational Methods

Our experimental method has been described in detail elsewhere.[49,50] In brief, a neodymium:yttrium−aluminum garnet (Nd:YAG) laser (1064 nm, 10 Hz repetition rate, 10 ns pulse width) was focused on a rotating transition metal target. Laser-ablated metal atoms were codeposited with benzene at 0.01−0.5% concentration in argon onto a CsI window cooled to 7 K, at 2−4 mmol/hour for 1 h. Benzene, isotopic samples (C_6D_6 (Cambridge Isotopic Laboratories; 99.6%), $^{13}C_6H_6$ (Cambridge Isotopic Laboratories; 99%)), and selected mixtures were purified through several freeze−pump−thaw cycles with liquid nitrogen before they were used in experiments. Fourier transform IR spectra were recorded at 0.5 cm^{-1} resolution on a Nicolet Magna 550 spectrometer with a mercury cadmium telluride type B detector cooled to 77 K with liquid nitrogen. Matrix samples were annealed to various temperatures (20−45 K) and subjected to broadband irradiation from a medium-pressure mercury arc lamp (Philips, 175 W) with the globe removed ($\lambda > 220$ nm).

Density functional theory (DFT) calculations were performed with the *Gaussian 98*[51] program. BPW91[52] and B3LYP[53] functionals were used for all calculations. The 6-311++G** basis set[54] was used for carbon and hydrogen atoms, while the SDD pseudopotential[55] was used to represent the transition metal

* E-mail: lsa@virginia.edu.

10.1021/jp046014z CCC: $30.25
Published on Web 12/30/2004

TABLE 1: Observed and Calculated Isotopic Frequencies (cm^{-1}) and Intensities (km/mol) at Different Levels for the $V(C_6H_6)$ and $V(C_6H_6)_2$ Complexes

BPW91/6-311++G**/SDD

			C_6H_6			C_6D_6			$^{13}C_6H_6$		
symmetry	species	mode[a]	obsd	calcd	int.	obsd	calcd	int.	obsd	calcd	int.
A_1	$V(C_6H_6)$[b]	ν_{o-p}(CH)	738.4	742.9	(160)	591.8	599.7	(87)	733.6	737.5	(158)
A_1		ν_s(CC)	942.3	936.5	(4)	899.3	896.2	(5)	909.3	903.1	(3)
E_1		ν_{i-p}(CH)	967.4	953.6	(41)	781.9	764.8	(19)	944.6	932.6	(40)
E_1		ν(CC)		1365.1	(5)	1229.0	1205.5	(22)		1340.9	(3)
A_{2u}	$V(C_6H_6)_2$[c]	ν_a(MC)	436.8	424.4	(133)	406.4	394.7	(137)	433.2	421.4	(130)
E_{1u}		ν_t(MC)	475.5	460.7	(25)	462.8	449.8	(27)	468.7	453.6	(24)
A_{2u}		ν_{o-p}(CH)	743.2	741.3	(92)	580.4	579.4	(8)	739.1	737.3	(95)
E_{1u}		$\nu_{o-p'}$(CH)	804.8	798.0	(7)		614.4	(1)	799.4	737.5	(7)
A_{2u}		ν_s(CC)	958.6	949.7	(40)	915.6	907.2	(39)	925.3	916.0	(35)
E_{1u}		ν_{i-p}(CH)	991.1	983.9	(19)	793.2	782.4	(9)	969.5	963.0	(18)
E_{1u}		ν(CC)	1419.1	1406.3	(1)		1249.3	(2)	1395.1	1380.2	(2)

B3LYP/6-311++G**/SDD

			C_6H_6			C_6D_6			$^{13}C_6H_6$		
symmetry	species	mode[a]	obsd	calcd	int.	obsd	calcd	int.	obsd	calcd	int.
A_1	$V(C_6H_6)$[b]	ν_{o-p}(CH)	738.4	766.4	(170)	591.8	607.3	(77)	733.6	761.4	(168)
A_1		ν_s(CC)	942.3	953.7	(4)	899.3	912.1	(5)	909.3	919.7	(3)
E_1		ν_{i-p}(CH)	967.4	976.7	(47)	781.9	784.9	(23)	944.6	954.9	(46)
E_1		ν(CC)		1413.7	(7)	1229.0	1244.1	(26)		1389.2	(4)
A_{2u}	$V(C_6H_6)_2$[c]	ν_a(MC)	436.8	411.6	(157)	406.4	388.5	(160)	433.2	408.5	(154)
E_{1u}		ν_t(MC)	475.5	460.0	(25)	462.8	448.8	(26)	468.7	452.9	(24)
A_{2u}		ν_{o-p}(CH)	743.2	759.4	(92)	580.4	584.9	(9)	739.1	755.7	(96)
E_{1u}		$\nu_{o-p'}$(CH)	804.8	825.2	(5)		636.7	(1)	799.4	819.6	(6)
A_{2u}		ν_s(CC)	958.6	971.3	(48)	915.6	927.7	(45)	925.3	936.8	(43)
E_{1u}		ν_{i-p}(CH)	991.1	1008.6	(21)	793.2	803.8	(10)	969.5	987.2	(20)
E_{1u}		ν(CC)	1419.1	1453.1	(1)		1287.2	(2)	1395.1	1426.5	(2)

[a] Vibrational modes: ν_a(MC) = asymmetric metal−carbon mode: ν_t(MC) = asymmetric tilting; ν_{o-p}(CH) = C−H out-of-plane bending; $\nu_{o-p'}$(CH) = C−H out-of-plane bending; ν_s(CC) = symmetric C−C stretching; ν_{i-p}(CH) = C−H in-plane rocking; ν(CC) = asymmetric C−C stretching. [b] Theoretical results: $^2A_1$ ground electronic state (C_{6v} symmetry). [c] Theoretical results: $^2A_{1g}$ ground electronic state (D_{6h} symmetry).

atoms. Geometries were optimized within specific symmetry constraints, and frequencies were calculated from second derivatives. Except where noted, energies are reported with zero-point vibrational corrections.

Results

Reactions of group 5 metal atoms with benzene will be reported in turn.

V + C_6H_6/Ar. Laser-ablated V atoms were codeposited with benzene diluted in argon. Different concentrations of benzene ranging from 0.01% to 0.5% were used. Two groups of absorptions were observed as new reaction products and are listed in Table 1, and spectra are shown in Figures 1−3. Group A bands at 738.4, 942.3, and 967.4 cm^{-1} appeared on deposition, increased on annealings up to 30 K and decreased on further annealings, and are labeled as VA in the figures. This group is favored in experiments with low benzene concentrations. Group B bands at 436.8, 475.5, 743.2, 804.8, 958.6, 991.1, and 1419.1 cm^{-1} are favored in experiments with high benzene concentrations. These bands appeared on deposition and increased on all annealings up to 45 K, and are labeled as VA_2 in the figures. An absorption at 935.7 cm^{-1} is common to all vanadium experiments. It arises from the extremely strong antisymmetric stretching mode of VO_2 produced by reactions with trace air contamination in our argon.[56] A very weak VN_2 band is also observed at 1709.1 cm^{-1}.[57]

Carbon-13 and deuterium isotopic counterparts of new product absorptions are also listed in Table 1. Spectra using C_6D_6, $^{13}C_6H_6$, and mixed C_6H_6 and C_6D_6 were recorded to help identify molecular stoichiometries and vibrational mode assignments.

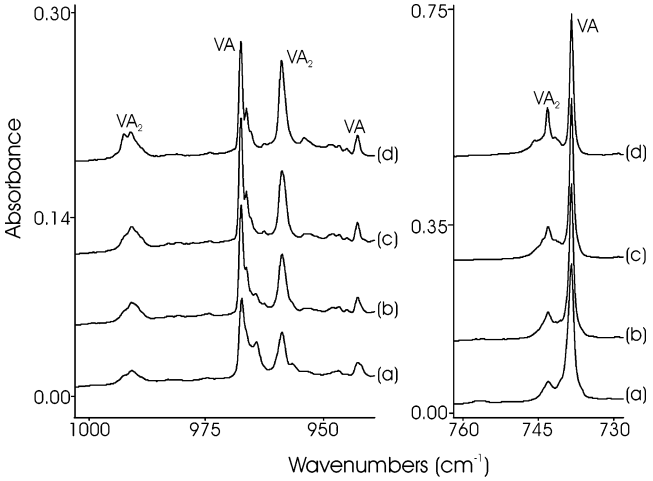

Figure 1. IR spectra in the 1000−940 and 760−730 cm^{-1} regions for (a) laser-ablated vanadium codeposited with benzene for 1 h and after annealing to (b) 30 K, (c) 35 K, and (d) 40 K. Absorptions labeled VA refer to the $V(C_6H_6)$ product, and absorptions labeled VA_2 refer to the $V(C_6H_6)_2$ species.

Nb + C_6H_6/Ar. Ranges of benzene concentrations (0.2−0.5% in argon) were codeposited with laser-ablated niobium atoms. The new IR product absorptions were placed into one of two groups based on product behavior. Group A bands at 748.5, 936.8, 957.8, and 1384.9 cm^{-1} appeared on deposition, increased in intensity on annealings up to 35 K, decreased slightly after broadband photolysis, and decreased upon further annealings. Group A bands were also favored in experiments with low concentrations of benzene and are labeled NbA in the figures. Group B absorptions at 731.1, 949.4, and 987.9 cm^{-1} appeared on deposition and increased on all annealings up to 40 K. Group

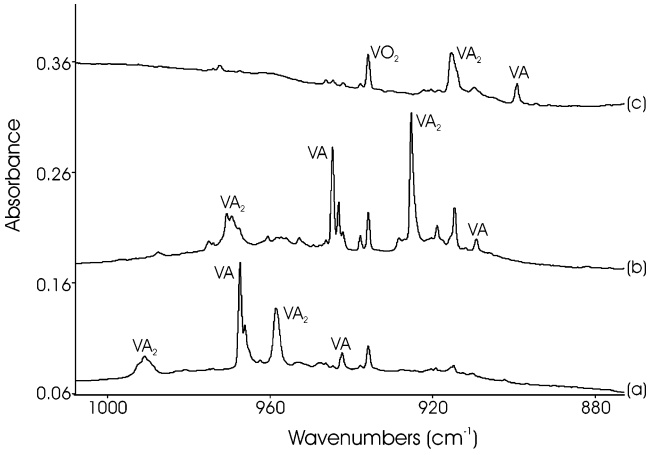

Figure 2. IR spectra in the 1000−880 cm^{-1} region from codepositing laser-ablated vanadium with (a) C_6H_6, (b) $^{13}C_6H_6$, and (c) C_6D_6 for 1 h. Spectra recorded after annealing to 35 K. Absorptions labeled VA refer to the $V(C_6H_6)$ product, and VA_2 corresponds to the $V(C_6H_6)_2$ product.

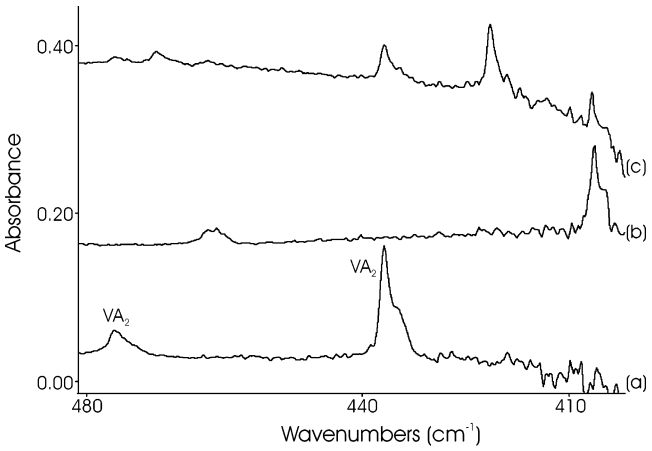

Figure 3. IR spectra in the 480−400 cm^{-1} region of the $V(C_6H_6)_2$ product formed when laser-ablated vanadium reacted with (a) 0.5% C_6H_6, (b) 0.5% C_6D_6, and (c) a mixture of 0.2% C_6H_6 and 0.2% C_6D_6 in argon. Spectra recorded after annealing to 35 K.

B bands are favored with high benzene concentrations, and are labeled NbA_2 in the figures. Experimental and theoretical vibrational results are summarized in Table 2, and spectra are show in Figures 4 and 5. Isotopic C_6D_6 and $^{13}C_6H_6$ reagents were used and spectra recorded to aid in vibrational mode identifications. Previously identified impurity absorptions were detected at 875.8 and 933.3 cm^{-1} (ONbO), 1888.7 cm^{-1} ($Nb(N_2)$), and 1914.4 cm^{-1} (NbNN).[58,59]

Ta + C_6H_6/Ar. Benzene (0.1−0.5%) was codeposited with laser-ablated Ta atoms in an argon matrix. From the behavior on annealing the matrix, the IR spectra show that two new complexes form simultaneously. Group A absorptions appeared at 753.9, 927.8, and 949.4 cm^{-1} on deposition, increased upon annealings to 35 K, decreased by $^1/_3$ after broadband photolysis, and then increased again on subsequent annealings. These absorptions were favored in reactions with lower concentrations of benzene, and are labeled TaA in the figures. Group B bands at 735.4 and 981.0 cm^{-1} were favored with higher benzene concentrations. They appeared on deposition and showed little or no change in appearance throughout the experiment, and are labeled TaA_2 in the figures. Observed vibrational absorptions are compared with theoretical results in Table 3, and spectra are shown in Figures 6 and 7. Isotopes of the benzene precursor (C_6D_6 and $^{13}C_6H_6$) were also employed. A weak absorption at 907.0 cm^{-1} is due to the TaO_2 molecule.[58]

Discussion

$V(C_6H_6)_x$ (x = 1, 2). IR spectra of the reaction products between vanadium and benzene in an argon matrix have been previously reported,[16] and the IR spectra of the $V(C_6H_6)_2$ compound has been studied extensively, as shown in Table 4. What follows is only enough to confirm our product identifications, explain the differences between our experimental results and those previously reported, and discuss new insights gained from $^{13}C_6H_6$ substitution. Two absorptions at 436.8 and 475.5 cm^{-1} show group B behavior and have deuterium counterparts at 406.4 and 462.8 cm^{-1}, which defines isotopic hydrogen H/D frequency ratios of 1.0748 and 1.0274, respectively. When experiments are performed with a mixture of C_6H_6 and C_6D_6 diluted in argon, both hydrogen and deuterium product absorptions are observed. In addition, a third absorption appears between the hydrogen and deuterium product absorptions for both of these modes at 421.4 and 469.9 cm^{-1}, respectively. For both of these vibrational modes, the three isotopic frequencies appear in a 1:2:1 relative intensity ratio, as shown in Figure 3. This indicates group B bands correspond to a bisbenzene complex. The absorption at 436.8 cm^{-1} is assigned to the antisymmetric metal−benzene ring mode (abbreviated ν_a(MC)), because it has a larger deuterium shift, and the absorption at 475.5 cm^{-1} is assigned to the antisymmetric tilting vibration (abbreviated ν_t(MC)). These assignments are opposite of those previously reported,[16] but are supported by this isotopic data. Knowing that group B absorptions correspond to a bisbenzene complex and that group A absorptions depend less on the benzene concentration, it follows that group A bands correspond to a monobenzene complex.

The carbon−hydrogen in-plane rocking vibration (abbreviated ν_{i-p}(CH)) of the $V(C_6H_6)$ product previously went undetected.[16] We observe a group A absorption at 967.4 cm^{-1} that shows an isotopic H/D frequency ratio of 1.2372 and a $^{12}C/^{13}C$ isotopic frequency ratio of 1.0241 (Figure 2), and we assign this absorption to ν_{i-p}(CH) of the $V(C_6H_6)$ product.

The symmetric breathing mode of the benzene precursor is IR inactive. However, this vibration is expected to become IR active as the benzene molecule binds to a metal atom. Previously, a frequency of 958 cm^{-1} was reported for this carbon−carbon symmetric stretching vibration (abbreviated ν_s(CC)) for both the mono- and bisbenzene complexes.[16] We observe this frequency at 958.6 cm^{-1} with type B product behavior. Note that the IR active ν_s(CC) mode of the $V(C_6H_6)_2$ product includes one of the benzene ligands expanding, while the other is compressing. However, as shown in Figure 1, a different absorption at 942.3 cm^{-1} shows type A behavior. The H/D (1.0478) and $^{12}C/^{13}C$ (1.0363) isotopic frequency ratios for this group A absorption are consistent with a ν_s(CC) mode, as the $V(C_6H_6)_2$ ν_s(CC) shows H/D and $^{12}C/^{13}C$ ratios of 1.0470 and 1.0360, respectively. We assign this absorption at 942.3 cm^{-1} to the ν_s(CC) stretching mode of the $V(C_6H_6)$ product.

Only one absorption appears in the region where the C−H stretching motions are expected at 3063.2 cm^{-1}. No isotopic counterpart of this absorption could be observed, and it is believed the other IR active modes in this region are hidden by the IR active C−H stretching vibrations and various combination bands of the benzene precursor that lie between 3045 and 3100 cm^{-1}. Previously, this absorption was identified at 3062 cm^{-1} as the symmetric CH stretching vibrations (abbreviated ν_s(CH)) of both the $V(C_6H_6)$ and $V(C_6H_6)_2$ molecules.[16] Although the

TABLE 2: Observed and Calculated Isotopic Frequencies (cm^{-1}) and Intensities (km/mol) at Different Levels of Theory for the $Nb(C_6H_6)$ and $Nb(C_6H_6)_2$ Complexes

BPW91/6-311++G**/SDD

			C_6H_6			C_6D_6			$^{13}C_6H_6$		
symmetry	species	mode[a]	obsd	calcd	int.	obsd	calcd	int.	obsd	calcd	int.
A_1	$Nb(C_6H_6)$[b]	ν_{o-p}(CH)	748.5	743.7	(109)	588.3	584.8	(58)	743.8	738.8	(108)
A_1		ν_s(CC)	936.8	923.8	(2)	893.8	883.1	(4)	903.9	890.9	(2)
E_1		ν_{i-p}(CH)	957.8	943.8	(33)	773.9	758.1	(17)	935.0	922.7	(32)
E_1		ν(CC)	1384.9	1360.0	(3)	1222.4	1197.5	1(5)		1336.4	(1)
A_{2u}	$Nb(C_6H_6)_2$[c]	ν_{o-p}(CH)	731.1	720.4	(86)	554.6	546.1	(16)	726.9	717.0	(90)
A_{2u}		ν_s(CC)	949.4	941.1	(50)	908.4	898.1	(51)	916.1	907.5	4(4)
E_{1u}		ν_{i-p}(CH)	987.9	975.4	(21)	787.6	776.4	(11)	965.8	954.4	(19)

B3LYP/6-311++G**/SDD

			C_6H_6			C_6D_6			$^{13}C_6H_6$		
symmetry	species	mode[a]	obsd	calcd	int.	obsd	calcd	int.	obsd	calcd	int.
A_1	$Nb(C_6H_6)$[b]	ν_{o-p}(CH)	748.5	772.6	(111)	588.3	600.7	(60)	743.8	767.8	(110)
A_1		ν_s(CC)	936.8	943.7	(3)	893.8	901.6	(5)	903.9	910.0	(2)
E_1		ν_{i-p}(CH)	957.8	968.4	(38)	773.9	779.5	(19)	935.0	946.5	(36)
E_1		ν(CC)	1384.9	1410.2	(4)	1222.4	1237.6	(18)		1386.1	(2)
A_{2u}	$Nb(C_6H_6)_2$[c]	ν_{o-p}(CH)	731.1	746.8	(82)	554.6	561.7	(16)	726.9	743.6	(85)
A_{2u}		ν_s(CC)	949.4	962.4	(61)	908.4	918.4	(61)	916.1	928.0	(54)
E_{1u}		ν_{i-p}(CH)	987.9	1002.1	(22)	787.6	799.1	(11)	965.8	980.5	(21)

[a] Vibrational Modes: ν_a(MC) = asymmetric metal−carbon mode; ν_t(MC) = asymmetric tilting; ν_{o-p}(CH) = C−H out-of-plane bending; $\nu_{o-p'}$(CH) = C−H out-of-plane bending; ν_s(CC) = symmetric C−C stretching; ν_{i-p}(CH) = C−H in-plane rocking; ν(CC) = asymmetric C−C stretching. [b] Theoretical results: $^2A_1$ ground electronic state (C_{6v} symmetry). [c] Theoretical results: $^2A_{1g}$ ground electronic state (D_{6h} symmetry).

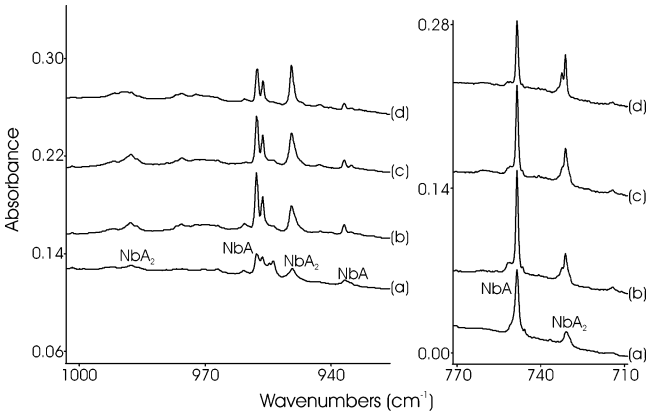

Figure 4. IR spectra in the 1000−930 and 770−710 cm^{-1} regions for (a) laser-ablated niobium codeposited with C_6H_6 for 1 h, (b) after annealing to 35 K, (c) after 20 min broadband photolysis, and (d) after annealing to 40 K. Absorptions labeled NbA refer to the $Nb(C_6H_6)$ product, and NbA_2 corresponds to the $Nb(C_6H_6)_2$ product.

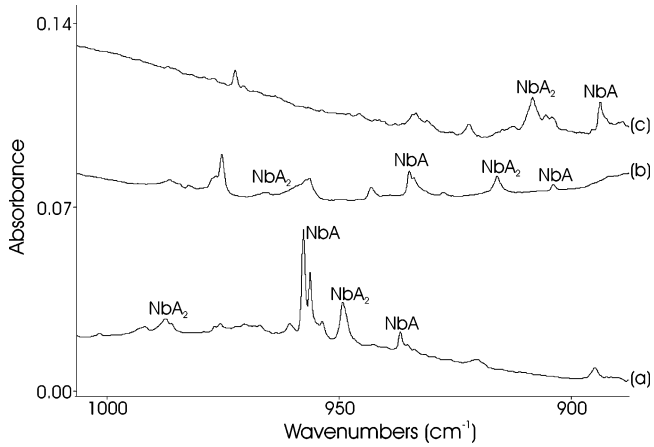

Figure 5. IR spectra in the 1000−890 cm^{-1} region from codepositing laser-ablated niobium with (a) C_6H_6, (b) $^{13}C_6H_6$, and (C) C_6D_6 for 1 h. Spectra recorded after annealing to 30 K. Absorptions labeled NbA refer to the $Nb(C_6H_6)$ product, and NbA_2 corresponds to the $Nb(C_6H_6)_2$ product.

antisymmetric C−H stretching vibration (abbreviated ν(CH)) was not observed in an Ar matrix, it was observed in a KBr pellet lower in frequency by about 135 cm^{-1} than the ν_s(CH) mode and with a lower relative intensity.[16] However, because this weak absorption is between stronger absorptions of the benzene precursor, it is difficult to characterize, and hence, we are unable to assign this absorption to a particular species or mode.

$Nb(C_6H_6)_x$ (x = 1, 2). As mentioned in the Introduction, when niobium was previously reacted with C_6H_6 in a matrix environment, only the $Nb(C_6H_6)_2$ product was observed.[33] In what follows, we compare our results to this study and provide evidence for the formation of the $Nb(C_6H_6)$ intermediate product.

The group A absorption at 748.5 cm^{-1} shows isotopic frequency ratios of 1.2725 (H/D) and 1.0063 ($^{12}C/^{13}C$). A group B absorption at 731.1 cm^{-1} shows a larger deuterium shift and a smaller carbon-13 shift than this absorption at 748.5 cm^{-1}. These absorptions are in the region where we expect the C−H out-of-plane bending vibration (abbreviated ν_{o-p}(CH)) of the product molecules to be observed. Previously, these absorptions were observed at 732 and 750 cm^{-1} in an argon matrix.[33] In this study, both of these absorptions were assigned to the $Nb(C_6H_6)_2$ complex. However, in our matrix, these absorptions show different behavior, as shown in Figure 4. In addition, our BPW91 and B3LYP calculations of the $Nb(C_6H_6)_2$ complex both predict only one vibrational mode in this region to have an IR intensity greater than 0.5 km/mol, at 720.4 and 746.8 cm^{-1}, respectively. Hence, we believe that these two absorptions belong to different reaction products. The observed isotopic shifts are consistent with the group B absorption corresponding to the $Nb(C_6H_6)_2$ product and the group A absorption belonging to the $Nb(C_6H_6)$ product, as illustrated by the experimental results of the vanadium and benzene experiment (see Table 1). It is of interest to note that the absorption at 748.5 cm^{-1} for the $Nb(C_6H_6)$ product is blue-shifted by about 10 cm^{-1} from the $V(C_6H_6)$ absorption, whereas this absorption at 731.1 cm^{-1} is red-shifted by about 7 cm^{-1} from the $V(C_6H_6)_2$ ν_{o-p}(CH) bending vibration.

TABLE 3: Observed and Calculated Isotopic Frequencies (cm^{-1}) and Intensities (km/mol) at Different Levels of Theory for the $Ta(C_6H_6)$ and $Ta(C_6H_6)_2$ Complexes

BPW91/6-311++G**/SDD

			C_6H_6			C_6D_6			$^{13}C_6H_6$		
symmetry	species	mode[a]	obsd	calcd	int.	obsd	calcd	int.	obsd	calcd	int.
A_1	$Ta(C_6H_6)$[b]	ν_{o-p}(CH)	753.9	736.3	(53)	586.2	573.1	(23)	751.3	731.6	(54)
A_1		ν_s(CC)	927.8	912.9	(9)	886.6	873.1	(11)		880.2	(8)
E_1		ν_{i-p}(CH)	949.4	932.1	(29)	769.1	752.0	(13)	929.6	910.7	(28)
E_1		ν(CC)		1344.3	(2)	1209.5	1178.7	(14)		1321.7	(1)
A_{2u}	$Ta(C_6H_6)_2$[c]	ν_{o-p}(CH)	735.4	723.9	(98)	546.2	546.8	(27)	729.4	720.4	(102)
A_{2u}		ν_s(CC)		937.7	(55)	905.0	894.6	(58)	913.3	904.2	(48)
E_{1u}		ν_{i-p}(CH)	981.0	971.1	(22)	785.3	773.7	(12)	960.4	950.1	(21)

B3LYP/6-311++G**/SDD

			C_6H_6			C_6D_6			$^{13}C_6H_6$		
symmetry	species	mode[a]	obsd	calcd	int.	obsd	calcd	int.	obsd	calcd	int.
A_1	$Ta(C_6H_6)$[b]	ν_{o-p}(CH)	753.9	763.6	(35)	586.2	589.5	(13)	751.3	759.1	(36)
A_1		ν_s(CC)	927.8	931.2	(17	)886.6	890.2	(18)		897.8	(15)
E_1		ν_{i-p}(CH)	949.4	954.8	(33)	769.1	772.2	(15)	929.6	932.7	(32)
E_1		ν(CC)		1393.1	(3)	1209.5	1217.1	(17)		1370.1	(2)
A_{2u}	$Ta(C_6H_6)_2$[c]	ν_{o-p}(CH)	735.4	750.3	(90)	546.2	563.5	(23)	725.9	746.9	(94)
A_{2u}		ν_s(CC)		959.1	(67)	905.0	915.0	(69)	913.3	924.8	(60)
E_{1u}		ν_{i-p}(CH)	981.0	995.9	(24)	785.3	795.2	(13)	960.4	974.2	(22)

[a] Vibrational Modes: ν_a(MC) = asymmetric metal−carbon mode; ν_t(MC) = asymmetric tilting; ν_{o-p}(CH) = C−H out-of-plane bending; $\nu_{o-p'}$(CH) = C−H out-of-plane bending; ν_s(CC) = symmetric C−C stretching; ν_{i-p}(CH) = C−H in-plane rocking; ν(CC) = asymmetric C−C stretching. [b] Theoretical results: $^2A_1$ ground electronic state (C_{6v} symmetry). [c] Theoretical results: $^2A_{1g}$ ground electronic state (D_{6h} symmetry).

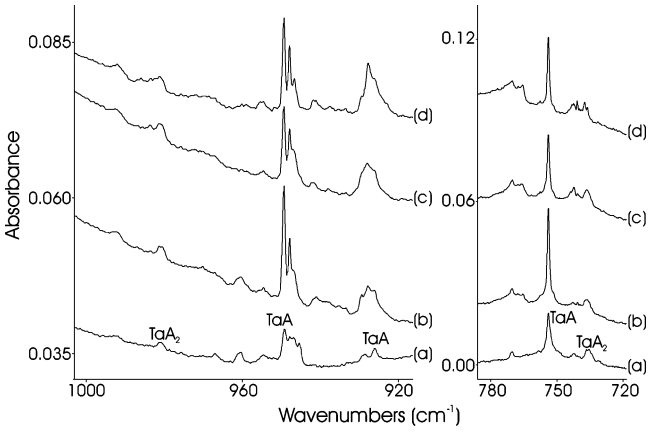

Figure 6. IR spectra in the 1000−920 and 780−720 cm^{-1} regions for (a) laser-ablated tantalum codeposited with C_6H_6 for 1 h, (b) after annealing to 35 K, (c) after photolysis for 20 min, and (d) after annealing to 40 K. Absorptions labeled TaA refer to the $Ta(C_6H_6)$ product, and TaA_2 corresponds to the $Ta(C_6H_6)_2$ product.

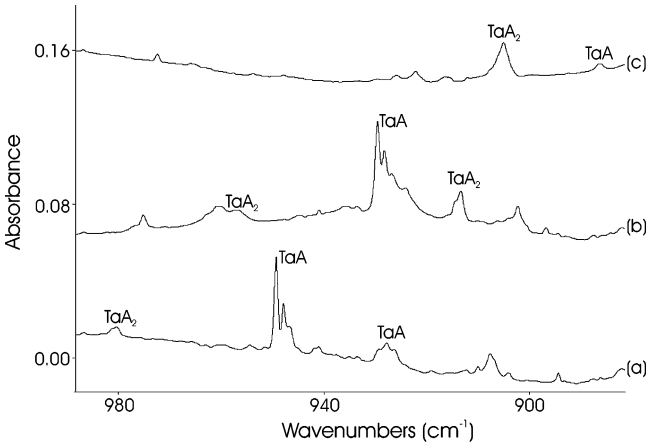

Figure 7. IR spectra in the 980−880 cm^{-1} region for the reaction products between laser-ablated tantalum and (a) C_6H_6, (b) $^{13}C_6H_6$, and (C) C_6D_6. Absorptions labeled TaA refer to the $Ta(C_6H_6)$ product, and TaA_2 corresponds to the $Ta(C_6H_6)_2$ product.

The group A absorption at 936.8 cm^{-1} shows a large carbon-13 shift and relatively small deuterium shift ($^{12}C/^{13}C = 1.0364$; H/D = 1.0481) indicating that this mode corresponds to a ν_s-(CC) stretching motion. The group B absorption at 949.4 cm^{-1} also shows a large carbon-13 shift and relatively small deuterium shift ($^{12}C/^{13}C = 1.0363$; H/D = 1.0451), also indicating a ν_s(CC) stretching motion. This absorption was previously observed at 950 cm^{-1} for the $Nb(C_6H_6)_2$ compound.[33] The group B absorption is observed at a higher frequency and shows slightly smaller H/D and $^{12}C/^{13}C$ ratios compared with the group A absorption. This trend is exactly what was observed for the ν_s(CC) mode of the $V(C_6H_6)_2$ and $V(C_6H_6)$ products, providing further evidence to support our assignment of the $Nb(C_6H_6)$ molecule to group A absorptions. These absorptions at 936.8 and 949.4 cm^{-1} are assigned to the ν_s(CC) stretching modes of the $Nb(C_6H_6)$ and $Nb(C_6H_6)_2$ molecules, respectively.

An absorption at 957.8 cm^{-1} shows group A behavior with an isotopic H/D ratio of 1.2375, and a group B absorption at 987.9 cm^{-1} shows an isotopic H/D ratio of 1.2543. The group B absorption is in good agreement with a previously observed absorption at 988 cm^{-1} assigned to the $Nb(C_6H_6)_2$ compound.[33] As in the vanadium experiment, we expect the ν_{i-p}(CH) vibration of the $Nb(C_6H_6)_2$ molecule to be at a higher frequency than the vibration of the $Nb(C_6H_6)$ product and with a larger H/D isotopic ratio. This is observed and provides further support for our molecular assignments.

An absorption observed at 1384.9 cm^{-1} shows group A behavior. The only vibrational mode that is expected in this region of the spectrum is the C−C antisymmetric stretch (abbreviated ν(CC)). In the vanadium experiment, the ν(CC) vibration of the $V(C_6H_6)$ product was not observed, but its deuterium counterpart was observed at 1229.0 cm^{-1}. This trend was reversed for the $V(C_6H_6)_2$ bisbenzene product. This absorption at 1384.9 cm^{-1} shifts to 1222.4 cm^{-1} and becomes more intense when the experiment is repeated with deuterated benzene. Hence, it is assigned to the ν(CC) vibration of the $Nb(C_6H_6)$ product. It should be noted that this C−C stretching mode of the $Nb(C_6H_6)_2$ molecules was also previously unseen in experiments.[33] An absorption at 3061.3 cm^{-1} could not be

TABLE 4: Comparison of the Theoretical and Experimental Bond Lengths (Å) and Vibrational Frequencies (cm^{-1}) for the $V(C_6H_6)_2$ Molecule

method	d_{V-C}	d_{V-Bz}[a]	d_{C-C}	d_{C-H}	ν_a(MC)	ν_t(MC)	ν_{o-p}(CH)	ν(C−C)	ν_{i-p}(CH)	ref
HF		1.708	1.411	1.072						5
MP2		1.565	1.438	1.088						5
B3LYP		1.675	1.426	1.084						5
B3P86		1.676	1.427	1.09						14
B3LYP	2.24									9
BPW91[b]		1.69	1.44	1.09						15
BPW91[c]		1.67	1.43	1.09						15
norm. coord.					463[d]	493[d]	796			3
norm. coord.					430	472	742	963	995	60
B3LYP								971		7
BPW91	2.199	1.671	1.428	1.089	424.4	460.7	741.3	949.7	983.9	this work
B3LYP	2.211	1.694	1.421	1.082	411.6	460.0	759.4	971.3	1008.6	this work
expt (solid)	2.17	1.66								61, 62
expt (solid)					429[d]	478[d]	742			3, 62, 63
expt (soln.)					430	473	745	960	992	60
expt (N_2)					434	472	743/747	958	991	17
expt (KBr)					424	470	742	957	988	16, 64
expt (Ar)							748	958	990	7
expt (Ar)					434[d]	471[d]	742	958	988	16
expt (Ar)					436.8	475.5	743.2	958.6	991.1	this work

[a] Distance calculated between the vanadium atom and the center of the benzene ring. [b] LanL2DZ basis set. [c] 6-311G** basis set. [d] The ν_a(MC) and the ν_t(MC) vibrational modes are assigned in the opposite order.

identified for the same reasons described for the vanadium products. However, we believe that this absorption is the same vibrational mode as the absorption at 3063.2 cm^{-1} observed in the vanadium experiment.

$Ta(C_6H_6)_x$ ($x = 1, 2$). The group A vibration at 753.9 cm^{-1} showed isotopic frequency ratios of 1.2861 and 1.0033 for H/D and $^{12}C/^{13}C$, respectively, and the group B absorption at 735.4 cm^{-1} has isotopic vibrational ratios of 1.3464 and 1.0082 (H/D and $^{12}C/^{13}C$, respectively). Both of these vibrations are in the region where we would expect the product ν_{o-p}(CH) bending vibrations to appear. The group B vibration shows a larger H/D ratio, which is consistent with this absorption for the $Ta(C_6H_6)_2$ product and the group A absorption for the monobenzene $Ta(C_6H_6)$ product. In this case, the ν_{o-p}(CH) modes of both the $Ta(C_6H_6)$ and the $Ta(C_6H_6)_2$ molecules are blue-shifted slightly from the niobium product absorptions. We note that previous attempts to obtain a matrix isolation IR spectra of this $Ta(C_6H_6)_2$ molecule have failed.[33]

Two group A absorptions observed at 927.8 and 949.4 cm^{-1} show drastically different H/D isotopic ratios (1.0465 and 1.2344, respectively). An absorption showed group B behavior at 981.0 cm^{-1} (H/D = 1.2492). These absorptions are consistent with ν_s(CC) and ν_{i-p}(CH) vibrational modes. Although the ν_s(CC) mode of the $Ta(C_6H_6)_2$ complex went undetected, the carbon-13 (913.3 cm^{-1}) and deuterium (905.0 cm^{-1}) isotopic counterparts were observed. Knowing the expected isotopic shifts for this vibrational mode in similar products, we expect this vibration to appear in the region where the ν_{i-p}(CH) vibrational mode of $Ta(C_6H_6)$ appears at 949.4 cm^{-1}, and it is probable that these two absorptions overlap. The ν_{i-p}(CH) vibration of the monobenzene product shows a smaller H/D ratio than the sandwich $Ta(C_6H_6)_2$ molecule. Also, for the $Ta(C_6H_6)$ product, the ν_{i-p}(CH) vibration is at a higher frequency than the ν_s(CC) mode. These trends are consistent with those observed for the niobium and vanadium products and provides more support for the assignment of the group A absorptions to the $Ta(C_6H_6)$, and the group B absorptions to the $Ta(C_6H_6)_2$ molecule.

Although the ν(CC) antisymmetric stretching vibration of the monobenzene complex was not observed, we believe the deuterium counterpart was observed at 1209.5 cm^{-1}, as it shows group A behavior. This vibrational mode was also not observed in the vanadium reaction, but its deuterium counterpart was found. An absorption at 3059.8 cm^{-1} is not identified for reasons already discussed. As mentioned previously, this absorption probably corresponds to one of the C−H stretches of either the $Ta(C_6H_6)$ or $Ta(C_6H_6)_2$ complexes.

Electronic Ground States and Geometries. DFT calculations were performed to support molecular identification. Calculations were performed on the $V(C_6H_6)$, $V(C_6H_6)_2$, $Nb(C_6H_6)$, $Nb(C_6H_6)_2$, $Ta(C_6H_6)$, and $Ta(C_6H_6)_2$ complexes, as well as on individual transition metal atoms and the benzene precursor. The geometries and spin multiplicities of the sandwich $M(C_6H_6)_2$ complexes have been well-characterized,[5,6,8−16,24,30] and we discuss our results for these molecules before the monobenzene complexes.

All previously reported theoretical and experimental results have confirmed that the $V(C_6H_6)_2$ molecule has a doublet ground electronic state with D_{6h} symmetry where the metal atom is sandwiched between the benzene rings.[5,6,8−16,24,30] Our DFT calculations also confirm a $^2A_{1g}$ ground state. We define ΔE_{rxn} as the calculated zero-point energy of the product molecule minus the calculated energy of the individual components (metal atom and benzene molecules). BWP91 calculations predicted a ΔE_{rxn} of −112 kcal/mol for this molecule, and B3LYP theoretical computations predicted a value of −95 kcal/mol. Our optimized geometrical parameters are compared to those previously reported in Table 4. It appears from the table that all theoretical predictions, with the exception of an MP2 calculation,[5] overestimate the length of the V−C bonds in this molecule. It is also observed from the vanadium−carbon bond length (V−C) and the distance from the vanadium atom to the center of the carbon ring (V−Bz) that our DFT results are comparable, and in some instances superior, to theoretical results previously reported for this molecule. A comparison of the vibrations of this molecule is also reported in Table 4. This table again shows that our theoretical methods are able to accurately predict the observed vibrational frequencies of this molecule. Earlier, we assigned the ν_a(MC) and ν_t(MC) absorptions of this molecule in the opposite order of previous reports.[3,16] However, we do see that our calculations predict the doubly degenerate antisymmetric tilting mode at a higher

frequency than the ν_a(MC) mode. In addition, our calculations predict the ν_a(MC) mode to have a larger H/D ratio, which is observed for the absorption at 436.8 cm^{-1} (Table 1).

As mentioned in the Introduction, considerably less is known about the monobenzene V(C_6H_6) molecule. It was first characterized as having a $^2A_1$ ground electronic state by theoretical and experimental methods.[16,27−29] Later theoretical studies indicated that a sextet electronic state was lower in energy.[10,31] Then, an electronic state with a spin multiplicity of four was presented as the ground electronic state for both short- and long-range geometries of the V(C_6H_6) molecule.[32] Most recently, the ground electronic state was again identified as a doublet state.[15] However, with the exception of one study,[15] these results have all assumed that the V(C_6H_6) molecule has C_{6v} symmetry. Our calculations with a $^2A_1$ ground electronic state converged in C_{6v} symmetry, and the geometry did not change drastically when we reduced the symmetry constraints. Our lowest energy sextet state was also found to have a $^6E_2$ ground state when constrained to the C_{6v} symmetry. However, calculations performed in a C_{2v} symmetry lowered the ground-state energy and showed a large deviation in the planarity of the benzene ring. Calculations performed in this C_{2v} symmetry led to our BPW91 method predicting a $^6B_1$ state and our B3LYP method predicting a $^6B_2$ state as the lowest-energy sextet state. However, the calculations in the $^6B_1$ ground electronic state produced a relatively large imaginary frequency, and it is assumed that the $^6B_2$ state is the lowest-lying sextet state. Calculations performed with a spin multiplicity of four also preferred the C_{2v} symmetry, and the $^4B_2$ state was predicted to be the lowest-lying quartet state. Our BPW91 calculations predicted the $^2A_1$ state to be 4 kcal/mol lower in energy than the quartet state and 9 kcal/mol lower in energy than the sextet state. However, our B3LYP calculations predicted the reverse order, with the sextet state predicted to be the most stable and the doublet to be the least. All of these electronic states were predicted by both theoretical methods to be less than 10 kcal/mol different in energy, and it is difficult to tell from these relative energy values the correct electronic ground state of this molecule. Although a complete computational analysis was obtained within C_{6v} and C_{2v} symmetry restraints, certain calculations produced a small imaginary frequency indicating the correct geometry might not have been found. In select instances, global C_1 calculations were performed to observe further deformations. Although these calculations produced slight variations of the geometry, the zero-point energies, vibrational frequencies, and isotopic shifts remained almost unchanged. Hence, we believe that computations constrained in the C_{6v} and C_{2v} symmetries produce results with an adequate level of accuracy for the M(C_6H_6) complexes in this study.

We expect our calculated frequencies to predict the observed values reasonably well, as these methods were shown to accurately predict the geometry and vibrations of the V(C_6H_6)$_2$ molecule. Any calculated vibrational errors should be consistent throughout our isotopic results, and we expect the vibrational isotopic ratios to be even more accurately predicted than the vibrational frequencies. The ν_{o-p}(CH) mode of the V(C_6H_6) molecule was observed at 738.4 with an H/D ratio of 1.2477. The H/D ratio for this mode of the calculated quartet and sextet states (1.3015 and 1.3497, respectively, for our BPW91 calculations) are both larger than those observed. However, the H/D ratio of the calculated doublet state (1.2388 and 1.2620 for BPW91 and B3LYP, respectively) reproduces the observed deuterium shift well. Also, our theoretical results for this ν_{o-p}(CH) mode of this molecule in the sextet state predicted this frequency at 700.1 and 722.0 cm^{-1} (BPW91 and B3LYP, respectively), considerably lower than the observed value of 738.4 cm^{-1}. The ν_s(CC) mode of this complex was observed at 942.3 cm^{-1} (H/D = 1.080). Theoretical results in the quartet state were unable to accurately reproduce these results, predicting this frequency at 919.9 and 938.2 cm^{-1} (BPW91 and B3LYP, respectively) with an H/D ratio of 1.0350. Our doublet-state results accurately predicted these vibrations and isotopic shifts as shown in Table 1. On the basis of this isotopic vibrational analysis, it is reasonable to conclude that the doublet state of the V(C_6H_6) complex forms in our matrix. EPR results have confirmed that this doublet state forms in an argon matrix,[16,27,29] showing that isotopic vibrational data can be used to identify the ground electronic state. Our BPW91 calculations predicted a ΔE_{rxn} of −39 kcal/mol of the V(C_6H_6) complex in the $^2A_1$ state, and B3LYP predicted a value of −30 kcal/mol.

Our theoretical results in this doublet state predicted a V−Bz distance of 1.503 and 1.535 Å (BPW91 and B3LYP, respectively), slightly larger than the values obtained in a previous study.[15] Our C−C bond lengths were calculated with the BPW91 (1.445 Å) and B3LYP (1.436 Å) methods compare better to the value of 1.45 Å than to 1.58 Å calculated with different basis sets by Kandalam et al.[15] We notice that our B3LYP calculations consistently predict longer V−C bond lengths and shorter C−C and C−H bond lengths regardless of the ground state when compared to our BPW91 calculations.

The bisbenzene Nb(C_6H_6)$_2$ and Ta(C_6H_6)$_2$ complexes have also been well-characterized.[9,14,24,33] Our calculations confined to a sandwich-like D_{6h} symmetry confirmed the $^2A_{1g}$ electronic ground state. Our theoretical and experimental vibrational results are shown in Tables 2 and 3. Again, we see good agreement between our theoretical and the observed values. ΔE_{rxn} was computed by the BPW91 method to be −118 kcal/mol for the Nb(C_6H_6)$_2$ molecule and −126 kcal/mol for the Ta(C_6H_6)$_2$ complex. Our B3LYP predictions gave different results: ΔE_{rxn} was calculated as −98 and −93 kcal/mol for the Nb(C_6H_6)$_2$ and Ta(C_6H_6)$_2$ complexes, respectively.

Our BPW91 computations predicted a distance from the metal atom to the center of the benzene rings of 1.870 Å for Nb(C_6H_6)$_2$ and 1.871 Å for the Ta(C_6H_6)$_2$ molecules. These correspond to M−C bond lengths of 2.355 and 2.356 Å for the Nb(C_6H_6)$_2$ and Ta(C_6H_6)$_2$ complexes, respectively. Our B3LYP calculations predicted longer M−Bz lengths of 1.899 and 1.894 Å for the Nb(C_6H_6)$_2$ and Ta(C_6H_6)$_2$ complexes, respectively. The M−C bond lengths are predicted to be 2.373 and 2.370 Å by our B3LYP calculations for the Nb(C_6H_6)$_2$ and Ta(C_6H_6)$_2$ complexes, respectively. Our Nb−C bond distance is in good agreement with the earlier prediction of 2.39 Å.[9] However, this previous study predicted a Ta−C bond length of 3.16 Å, considerably larger than our predictions. Given the only slightly larger atomic radius of tantalum, and that we believe tantalum binds more strongly to the benzene ring than niobium, it seems reasonable that the two M−C bond lengths should be similar. Indeed, our calculated geometries of both the Nb(C_6H_6)$_2$ and Ta(C_6H_6)$_2$ molecules are in better agreement with a previous study, which predicts a Nb−Bz distance of 1.873 Å and a Ta−Bz distance of 1.872 Å for these complexes.[14] Our computations did give longer M−Bz distances than that predicted for the V(C_6H_6)$_2$ complex, attributed to the increased atomic radius of the transition metal atoms. BPW91 calculations predicted an increase from 1.432 to 1.433 Å for the C−C bond length of the Nb(C_6H_6)$_2$ and Ta(C_6H_6)$_2$ complexes, respectively, from a value of 1.428 Å calculated for the V(C_6H_6)$_2$ complex. This indicates a weakening of the C−C bond as the metal atoms are

changed going down the group 5 family. These values can be compared with our BPW91 calculated C−C bond length of 1.401 Å and the experimental value of 1.390 Å for free benzene.[65] B3LYP calculations also predicted an increase in the C−C bond length while moving down the group 5 family from 1.421 to 1.423 to 1.425 Å for these sandwich compounds. Our B3LYP computations on free benzene gave a C−C bond length of 1.395 Å.

Calculations performed in the doublet state of the Nb(C_6H_6) complex converged to a $^2A_1$ ground electronic state within the C_{6v} symmetry constraint. Reducing this constraint did not alter the geometry significantly. Calculations performed in the quartet and sextet states for this molecule showed large geometrical deviations when converged in a C_{2v} symmetry. The $^4A_2$ state with C_{2v} symmetry was found to be the lowest-lying quartet state, which is interesting as this is a different state than the lowest-lying quartet state of the V(C_6H_6) complex. The $^6B_1$ and $^6B_2$ states with C_{2v} symmetry were both found to be the lowest-lying sextet states, with the $^6B_1$ state predicted to be slightly more stable by both theoretical methods. However, both the $^6B_1$ and the $^6B_2$ states produced small imaginary frequencies. We cannot say which of the $^6B_1$ or $^6B_2$ states is the lowest sextet state, but both were calculated to be significantly higher in energy than the doublet and quartet states. Our BPW91 calculations predicted the doublet $^2A_1$ state to be the ground electronic state, with the $^4A_2$ state being 11 kcal/mol higher in energy and the $^6B_1$ state lying 31 kcal/mol higher in energy. B3LYP calculations followed this trend, but gave slightly smaller relative energy differences. As the electron configuration of atomic niobium is different than that of vanadium (vanadium and tantalum take a d^3s^2 configuration, whereas niobium has a d^4s^1 electron distribution), it is quite possible that complexes of vanadium and niobium differ in their electronic ground states. However, this energy difference indicates that Nb(C_6H_6) does not assume the sextet state and that the doublet state is probably the ground electronic state.

Both of our theoretical methods predicted the ν_{o-p}(CH) mode between 676.0 and 722.4 cm^{-1} for both sextet states, with an H/D ratio of 1.356. These values poorly represent the observed vibration at 748.5 cm^{-1} (H/D = 1.2723). The quartet-state calculation also overestimated this H/D ratio, predicting values of 1.3064 and 1.3141 for the BPW91 and B3LYP methods, respectively. Calculations performed in the doublet state predicted this frequency at 743.7 (H/D = 1.2717) and 772.6 cm^{-1} (H/D = 1.2862) with the BPW91 and B3LYP methods, respectively, accurately reproducing the observed results for this mode. The experimental H/D ratio of the ν_s(CC) at 936.8 cm^{-1} was observed to be 1.0481. Theoretical results in the quartet state had difficulty reproducing this result, predicting H/D isotopic ratios of 1.0422 (BPW91) and 1.0400 (B3LYP). Calculations performed in the doublet state reproduced the observed results well, as shown in Table 2. Hence, we believe that the Nb(C_6H_6) complex takes this $^2A_1$ ground state in our matrix. By using the calculations for this doublet state, the ΔE_{rxn} was predicted to be −49 kcal/mol by our BPW91 calculations and −37 kcal/mol by the B3LYP method. Both of these values are larger than the ΔE_{rxn} for the V(C_6H_6) complex, and the niobium complex is favored more in this reaction.

The Nb−Bz distance of the Nb(C_6H_6) complex in the $^2A_1$ state was predicted by the BPW91 method to be 1.681 Å. Our B3LYP calculations predicted a value of 1.711 Å. Both of these predictions are longer than the V−Bz lengths in the V(C_6H_6) complex, which is again contributed to the increased atomic radius of niobium. Our calculations predicted a C−C bond length in the Nb(C_6H_6) complex of 1.449 Å using the BPW91 method and 1.440 Å using the B3LYP method. Both of these values are larger than that predicted for the V(C_6H_6) complex, indicating a weakening of the C−C bond.

The Ta(C_6H_6) molecule converged into a $^2A_1$ doublet state with C_{6v} symmetry. The quartet state preferred a C_{2v} geometry with the $^4A_2$ state having the lowest energy. The $^6B_2$ and $^6B_1$ states with C_{2v} symmetry were found to be the lowest-lying sextet states. Our BPW91 calculations predicted the $^6B_2$ state to be slightly more stable than the $^6B_1$ state, but our B3LYP calculations predicted the $^6B_1$ state to be at a lower energy. However, the $^6B_1$ state was predicted by the B3LYP method to have a large imaginary frequency. Again, we find that the sextet states are predicted to be considerably higher in energy than the doublet and quartet states. Our BPW91 calculations predicted the doublet state to be the most stable with the quartet state lying less than 1 kcal/mol higher in energy. The sextet states were predicted to be 26 kcal/mol higher in energy. However, our B3LYP calculations found the quartet state to be the most stable, with the doublet state slightly more than 1 kcal/mol higher in energy. The sextet states were again predicted to be significantly higher in energy (24 kcal/mol). The magnitude of the energy difference of the sextet state indicates that the Ta(C_6H_6) complex does not assume this electronic state. However, the doublet and quartet states are very close in energy, and both need to be considered as possibilities for the ground state of this complex.

In looking at the ν_{o-p}(CH) mode observed at 753.9 cm^{-1} (H/D = 1.2861), we see that again our theoretical isotopic results in the sextet (H/D = 1.35) and quartet (H/D = 1.31−1.32) states had trouble reproducing the observed isotopic shifts. The quartet state also had problems reproducing the observed H/D isotopic ratio (1.0465) of the ν_s(CC) mode, predicting values of 1.0409 and 1.0387 at the BPW91 and B3LYP levels, respectively. Calculations in the doublet state did an excellent job reproducing the observed results for both of these modes, as shown in Table 3. We believe the Ta(C_6H_6) molecule takes this $^2A_1$ ground state with C_{6v} symmetry in our argon matrix. The ΔE_{rxn} was predicted to be −49 kcal/mol by the BPW91 method, but only −25 kcal/mol by the B3LYP method. It is interesting that for both the mono- and bisbenzene products, the BPW91 method predicts the tantalum products to have the largest exothermic ΔE_{rxn} and be the most stabilized by the complexation, compared to the V and Nb compounds. However, the B3LYP method predicts these tantalum products to be the least stabilized by the complexation. For all the reaction products, ΔE_{rxn} is negative, predicting our products to be energetically favorable to form.

Our BPW91 calculations gave a Ta−Bz distance of 1.659 Å, and our B3LYP computations predicted a value of 1.686 Å for this Ta(C_6H_6) molecule. The tantalum atom has a slightly larger atomic radius than niobium, but our calculations predicted the tantalum atom to be closer to the benzene ring than niobium. This indicates that tantalum may bind more strongly to the benzene ring than niobium and vanadium. The C−C bond distance was computed to be 1.457 and 1.449 Å at the BPW91 and B3LYP levels, respectively. These C−C bond distances are longer than in the niobium complex, indicating a further weakening of the C−C bond.

Before the reaction with the metal atom occurs, the hydrogen atoms are in the plane of the carbon skeleton of benzene. BPW91 calculations predicted that the hydrogen atoms move in the monobenzene molecules toward the metal atom by 5.8°, 2.9°, and 3.0° when the transition metal is V, Nb, and Ta, respectively. For the M(C_6H_6)$_2$ complex, the hydrogen atoms

shifted out of the carbon plane by 2.7°, 0.2°, and 0.3° for vanadium, niobium, and tantalum, respectively. We see that these deviations are greater for the monobenzene species and that they are larger for vanadium than for the heavier group 5 metals. It should be noted that although our calculations predict the hydrogen atoms to move toward the metal atoms, other computational methods have predicted a movement away from the metal atom in the $V(C_6H_6)_2$ compound.[5]

Bonding Considerations. Previously, the observed shifts in the ν_s(CC) mode have been used to comment on the strength of the C−C bonds as well as the M−C bonds in metal−benzene complexes.[7,43] This method has also been used to observe periodic trends in transition metal−ethylene complexes.[66] The ν_s(CC) stretching frequencies red-shift as the metal atom is changed going down the group 5 transition metals for both the mono- and bisbenzene complexes. (Note that even though we did not observe the ν_s(CC) mode of the $Ta(C_6H_6)_2$ complex, we believe that it is covered by the ν_{i-p}(CH) mode of the $Ta(C_6H_6)$ molecule around 949 cm^{-1}.) This trend corresponds to a weakening of the C−C bond. Recall that our BPW91 calculated geometries predicted an increase in the C−C bond lengths from 1.445 to 1.449 to 1.457 Å (from V to Nb to Ta) for the monobenzene complex and from 1.428 to 1.432 to 1.433 Å, respectively, for the bisbenzene complex. It is reasonable to conclude that two simple interactions contribute to the bonding of the metal atoms to the benzene ring. The first is the donation of the benzene electrons from the bonding π-orbital to the unoccupied metal orbitals, and the second is the back-donation of the metal d-electrons to the unoccupied antibonding π*-orbital of benzene. Both of these interactions support the strengthening of the metal−carbon bonds as the carbon−carbon bonds weaken. Hence, the M−C bond strength increases down the group 5 transition metal column. The atomic transition metal d-orbital energies become less negative down the group 5 transition metal family, and the strength of the M−C bonds increase in the same direction. This suggests the primary electronic interaction responsible for the bonding is the back-donation of the transition metal electrons to the benzene ring. Previous studies also indicated back π-bonding as the primary electronic interactions in transition metal−benzene complexes.[7,43] If the interaction responsible for the bonding was the donation of the benzene π-electrons, the observed trend of metal−carbon bond strengths would be reversed.

Conclusions

The molecules that form in an argon matrix during the reactions between vanadium, niobium, and tantalum atoms and benzene have been studied by IR spectroscopy and DFT calculations. We conclude that the primary products are the $M(C_6H_6)$ and the sandwich $M(C_6H_6)_2$ complexes. DFT calculations predict the geometries and vibrational frequencies for these complexes. Comparing the observed and calculated isotopic frequencies and the calculated relative zero-point energies, we predict a $^2A_{1g}$ electronic ground state for the $M(C_6H_6)_2$ compounds and a $^2A_1$ ground state for the $M(C_6H_6)$ complexes. Periodic trends of the metal−carbon bond strengths are discussed by a comparison of the symmetric carbon−carbon stretching frequencies in the 900−1000 cm^{-1} region, which are confirmed by ^{13}C substitution. The primary electronic interaction responsible for the metal−benzene bonding is the back-donation of the transition metal d-electrons to the π* antibonding orbitals of benzene.

Acknowledgment. We gratefully acknowledge National Science Foundation (NSF) support for this research under grant CHE 00-78836, and fellowship support under NSF IGERT grant 9972797 for J.T.L.. We also thank C. O. Trindle for helpful discussions.

References and Notes

(1) Fischer, E. O.; Kögler, H. P. *Chem. Ber.* **1957**, *90*, 250.
(2) Hirano, M.; Judai, K.; Nakajoma, A.; Kaya, K. *J. Phys. Chem. A* **1997**, *101*, 4893.
(3) Cyvin, S. J.; Cyvin, B. N.; Brunvoll, J.; Schäfer, L. *Acta Chem. Scand.* **1970**, *24*, 3420.
(4) Froudakis, G. E.; Andriotis, A. N.; Menon, M. *Chem. Phys. Lett.* **2001**, *350*, 393.
(5) Yasuike, T.; Yabushita, S. *J. Phys. Chem. A* **1999**, *103*, 4533.
(6) Clack, D. W.; Smith, W. *Inorg. Chim. Acta* **1976**, *20*, 93.
(7) Judai, K.; Sera, K.; Amatsutsumi, S.; Yagi, K.; Yasuike, T.; Yabushita, S.; Nakajima, A.; Kaya, K. *Chem. Phys. Lett.* **2001**, *334*, 277.
(8) Andrews, M. P.; Mattar, S. M.; Ozin, G. A. *J. Phys. Chem.* **1986**, *90*, 1037.
(9) Rayane, D.; Allouche, A. R., Antoine, R.; Broyer, M.; Compagnon, I.; Dugourd, P. *Chem. Phys. Lett.* **2003**, *375*, 506.
(10) (a) Pandey, R.; Rao, B. K.; Jena, P.; Blanco, M. A. *J. Am. Chem. Soc.* **2001**, *123*, 3799. (b) Pandey, R.; Rao, B. K.; Jena, P.; Blanco, M. A. *J. Am. Chem. Soc.* **2001**, *123*, 7744.
(11) Fantucci, P.; Balzarini, P.; Valenti, V. *Inorg. Chim. Acta* **1977**, *25*, 113.
(12) Anderson, S. E.; Drago, R. S. *Inorg. Chem.* **1972**, *11*, 1564.
(13) Clack, D. W.; Warren, K. D. *Inorg. Chim. Acta* **1978**, *30*, 251.
(14) Dolg, M. *J. Chem. Inf. Comput. Sci.* **2001**, *41*, 18.
(15) Kandalam, A. K.; Rao, B. K.; Jena, P.; Pandey, R. *J. Chem. Phys.* **2004**, *120*, 10414.
(16) Andrews, M. P.; Mattar, S. M.; Ozin, G. A. *J. Phys. Chem.* **1986**, *90*, 744.
(17) McCamley, A.; Perutz, R. N. *J. Phys. Chem.* **1991**, *95*, 2738.
(18) Anderson, S. E., Jr.; Drago, R. S. *J. Am. Chem. Soc.* **1970**, *92*, 4244.
(19) Hoshino, K.; Kurikawa, T.; Takeda, H.; Nakajoma, A.; Kaya, K. *J. Phys. Chem.* **1995**, *99*, 3053.
(20) Kurikawa, T.; Takeda, H.; Nakajima, A.; Kaya, K. *Z. Phys. D* **1997**, *40*, 65.
(21) Kurikawa, T.; Takeda, H.; Hirano, M.; Judai, K.; Arita, T.; Nagao, S.; Nakajima, A.; Kaya, K. *Organometallics* **1999**, *18*, 1430.
(22) Nakajima, A.; Kaya, K. *J. Phys. Chem. A* **2000**, *104*, 176.
(23) Schweiger, A.; Wolf, R.; Günthard, Hs. H.; Ammeter, J. H.; Deiss, E. *Chem. Phys. Lett.* **1980**, *71*, 117.
(24) Cloke, F. G. N.; Dix, A. N.; Green, J. C.; Perutz, R. N.; Seddon, E. A. *Organometallics* **1983**, *2*, 1150.
(25) Ketkov, S. Yu.; Domrachev, G. A.; Razuvaev, G. A. *J. Mol. Struct.* **1989**, *195*, 175.
(26) Cirelli, G.; Russu, A.; Wolf, R.; Rudin, M.; Schweiger, A.; Günthard, Hs. H. *Chem. Phys. Lett.* **1982**, *92*, 223.
(27) Andrews, M. P.; Huber, H. X.; Mattar, S. M.; McIntosh, D. F.; Ozin, G. A. *J. Am. Chem. Soc.* **1983**, *105*, 6170.
(28) Mattar, S. M.; Hamilton, W. *J. Phys. Chem.* **1989**, *93*, 2997.
(29) Mattar, S. M.; Sammynaiken, R. *J. Chem. Phys.* **1997**, *106*, 1080.
(30) Yasuike, T.; Nakajima, A.; Yabushita, S.; Kaya, K. *J. Phys. Chem. A* **1997**, *101*, 5360.
(31) Pandey, R.; Rao, B. K.; Jena, P.; Newsam, J. M. *Chem. Phys. Lett.* **2000**, *321*, 142.
(32) Rabilloud, F.; Rayane, D.; Allouche, A. R.; Antoine, R.; Aubert-Frécon, M.; Broyer, M.; Compagnon, I.; Dugourd, Ph. *J. Phys. Chem. A* **2003**, *107*, 11347.
(33) Cloke, F. G. N.; Green, M, L. H. *J. Chem. Soc., Dalton Trans.* **1981**, 1938.
(34) Andrews, L.; Johnson, G. L.; Davis, S. R. *J. Phys. Chem.* **1985**, *89*, 1706.
(35) Engdahl, A.; Nelander, B. *J. Phys. Chem.* **1985**, *89*, 2860.
(36) Bai, H.; Ault, B. S. *J. Phys. Chem.* **1990**, *94*, 199.
(37) Manceron, L.; Andrews, L. *J. Am. Chem. Soc.* **1988**, *110*, 3840.
(38) Kim, H. S.; Kim, K. *Chem. Phys. Lett.* **1996**, *250*, 192.
(39) Engdahl, A.; Nelander, B. *J. Chem. Phys.* **1982**, *77*, 1649.
(40) Andrews, M. P.; Ozin, G. A. *J. Phys. Chem.* **1986**, *90*, 1245.
(41) Boyd, J. W.; Lavoie, J. M.; Gruen, D. M. *J. Chem. Phys.* **1974**, *60*, 4088.
(42) Shobert, A. L.; Hisatsune, I. C.; Skell, P. S. *Spectrochim. Acta* **1984**, *40A*, 609.
(43) Efner, H. F.; Tevault, D. E.; Fox, W. B.; Smardzewski, R. R. *J. Organomet. Chem.* **1978**, *146*, 45.
(44) Ball, D. W.; Kafafi, Z. H.; Hauge, R. H.; Margrave, J. L. *J. Am. Chem. Soc.* **1986**, *108*, 6621.
(45) Benfield, F. W. S.; Green, M. L. H.; Ogden, J. S.; Young, D. *J. Chem. Soc., Chem. Commun.* **1973**, 866.

(46) Anthony, M. T.; Green, M. L. H.; Young, D. *J. Chem. Soc., Dalton Trans.* **1975**, 1419.
(47) Brown, K. G.; Person, W. B. *Spectrochim. Acta* **1978**, *34A*, 117.
(48) Johnstone, D. E.; Sodeau, J. R. *J. Phys. Chem*. **1991**, *95*, 165.
(49) Zhou, M.; Andrews, L.; Bauschlicher, C. W., Jr. *Chem. Rev.* **2001**, *101*, 1931.
(50) Andrews, L.; Citra, A. *Chem. Rev.* **2002**, *102*, 885.
(51) Frisch, M. J.; Trucks, G. W.; Schlegel, H. B.; Scuseria, G. E.; Robb, M. A.; Cheeseman, J. R.; Zakrzewski, V. G.; Montgomery, J. A., Jr.; Stratmann, R. E.; Burant, J. C.; Dapprich, S.; Millam, J. M.; Daniels, A. D.; Kudin, K. N.; Strain, M. C.; Farkas, O.; Tomasi, J.; Barone, V.; Cossi, M.; Cammi, R.; Mennucci, B.; Pomelli, C.; Adamo, C.; Clifford, S.; Ochterski, J.; Petersson, G. A.; Ayala, P. Y.; Cui, Q.; Morokuma, K.; Malick, D. K.; Rabuck, A. D.; Raghavachari, K.; Foresman, J. B.; Cioslowski, J.; Ortiz, J. V.; Stefanov, B. B.; Liu, G.; Liashenko, A.; Piskorz, P.; Komaromi, I.; Gomperts, R.; Martin, R. L.; Fox, D. J.; Keith, T.; Al-Laham, M. A.; Peng, C. Y.; Nanayakkara, A.; Gonzalez, C.; Challacombe, M.; Gill, P. M. W.; Johnson, B. G.; Chen, W.; Wong, M. W.; Andres, J. L.; Head-Gordon, M.; Replogle, E. S.; Pople, J. A. *Gaussian 98*, revision A.11.4; Gaussian, Inc.: Pittsburgh, PA, 1998.
(52) (a) Becke, A. D. *Phys. Rev. A* **1988**, *38*, 3098. (b) Perdew, J. P.; Wang, Y. *Phys. Rev. B* **1992**, *45*, 13244.
(53) (a) Becke, A. D. *J. Chem. Phys.* **1993**, *98*, 5648. (b) Lee, C.; Yang, W.; Parr, R. G. *Phys. Rev. B* **1988**, *37*, 785.
(54) (a) Krishnan, F.; Binkley, J. S.; Seeger, R.; Pople, J. A. *J. Chem. Phys.* **1980**, 72, 650. (b) Frisch, M. J.; Pople, J. A.; Binkley, J. S. *J. Chem. Phys.* **1984**, *80*, 3265.
(55) Andrae, D.; Haussermann, U.; Dolg, M.; Stoll, H.; Preuss, H. *Theor. Chim. Acta* **1990**, *77*, 123.
(56) Chertihin, G. V.; Bare, W. D.; Andrews, L. *J. Phys. Chem. A* **1997**, *101*, 5090.
(57) Andrews, L.; Bare, W. D.; Chertihin, G. V. *J. Phys. Chem. A* **1997**, *101*, 8417.
(58) Zhou, M.; Andrews, L. *J. Phys. Chem. A* **1998**, *102*, 8251.
(59) Zhou, M.; Andrews, L. *J. Phys. Chem. A* **1998**, *102*, 9061.
(60) Greenwald, I. I.; Lokshin, B. V. *J. Mol. Struct.* **1990**, *218*, 255.
(61) Muetterties, E. L.; Bleeke, J. R.; Wucherer, E. J. *Chem. Rev.* **1982**, *82*, 499.
(62) Fischer, E. O.; Fritz, H. P.; Manchot, J.; Priebe, E.; Schneider, R. *Chem. Ber.* **1963**, *96*, 1418.
(63) Fritz, H. P.; Fischer, E. O. *J. Organomet. Chem.* **1967**, *7*, 121.
(64) Fritz, H. P.; Luttke, W.; Stammereich, H.; Foreris, R. *Spectrochim. Acta* **1961**, *17*, 1068.
(65) Pliva, J.; Johns, J. W. C.; Goodman, L. *J. Mol. Spectrosc.* **1991**, *148*, 427.
(66) Huber, H.; McIntosh, D.; Ozin, G. A. *J. Organomet. Chem.* **1976**, *112*, C50.